Novel SARS-CoV-2 specific antibody and neutralization assays reveal wide range of humoral immune response during COVID-19

Mikail Dogan[1], Lina Kozhaya[1], Lindsey Placek[1], Courtney L. Gunter[1], Mesut Yigit[1], Rachel Hardy[1], Matt Plassmeyer[3], Paige Coatney[3], Kimberleigh Lillard[3], Zaheer Bukhari[4], Michael Kleinberg[5], Chelsea Hayes[6], Moshe Arditi[7], Ellen Klappper[6], Noah Merin[8], Bruce T Liang[5], Raavi Gupta[4], Oral Alpan[3] and Derya Unutmaz[1,2]*

[1] Jackson Laboratory for Genomic Medicine, Farmington, Connecticut

[2] Department of Immunology, University of Connecticut School of Medicine, Farmington, CT

[3] Amerimmune, Fairfield, VA

[4] SUNY Downstate Medical Center, Department of Pathology, Brooklyn, NY

[5] Calhoun Cardiology Center, University of Connecticut School of Medicine, Farmington, CT.

[6] Department of Pathology & Laboratory Medicine and Transfusion Medicine
Cedars-Sinai Medical Center, Los Angeles, CA.

[7]Department of Pediatric, Division of Pediatric Infectious Diseases and Immunology, Biomedical Sciences, Cedars-Sinai Medical Center,
Los Angeles, CA 90048.

[8]Department of Internal Medicine, Division of Hematology Cedars-Sinai Medical Center, Los Angeles, CA.

* Corresponding author E-mail: derya@mac.com

Abstract

Development of antibody protection during SARS-CoV-2 (CoV-2) infection is a pressing question for public health and for vaccine development. We developed highly sensitive CoV-2-specific antibody and neutralization assays. CoV-2 Spike protein or Nucleocapsid protein specific IgG antibodies at titers more than 1:100,000 were detectable in all PCR+ subjects (n=87) and were absent in the negative controls. Other isotype antibodies (IgA, IgG1-4) were also detected. CoV-2 neutralization was determined in COVID-19 and convalescent plasma up to 10,000-fold dilution, using Spike protein pseudotyped lentiviruses, which was also blocked by neutralizing antibodies (NAbs). Hospitalized patients had up to 3000-fold higher antibody and neutralization titers compared to outpatients or convalescent plasma donors. Further, subjects who donated plasma further out from the diagnosis of COVID-19 appeared to have lower titers. Interestingly, some COVID-19 patients also contained NAbs against SARS Spike protein pseudovirus. Together these results demonstrate the high specificity and sensitivity of our assays, which may impact understanding the quality or duration of the antibody response during COVID-19 and in determining the effectiveness of potential vaccines.

Introduction

Severe Acute Respiratory Syndrome Coronavirus 2 (SARS-CoV-2; CoV-2), which has caused the COVID-19 pandemic, enters the target cells through the interaction of its envelope Spike protein with the primary host cell receptor Angiotensin Converting Enzyme-2 (ACE2), which is then cleaved by a serine protease (TMPRSS2) to allow viral fusion and entry across the cell membrane[1]. Antibodies that can bind to the Spike protein have the potential to neutralize viral entry into cells and are thought to play an important role in the protective immune response to CoV-2 infection[2-6]

To predict protection against CoV-2, it is critical to understand the quantity, quality and duration of the antibody responses during different stages of COVID-19 and in the convalescent period. In this regard, assessing the level of neutralizing antibodies (NAbs) that block viral entry into cells could be a critical parameter in determining protection from CoV-2 and management of convalescent plasma therapies, which are being tested as a COVID-19 treatment option[7-10]. Defining the relationship between the disease severity, other individual-specific co-morbidities and the neutralizing antibody responses will be critical in our understanding of COVID-19 and in tailoring effective therapies.

Currently available CoV-2 antibody tests lack dynamic range and sensitivity to allow for acurate detection or determining the magnitude of the antibody response[11]. Furthermore, potential cross-reactivity among CoV-2 specific antibodies to other endemic coronaviruses could also be confounders in these tests [12-15], thus making them less reliable. Determining neutralization activity in patient plasma also has challenges, as these assays generally rely on live virus replication, requiring a high-level biohazard security BSL-3 level laboratory. Therefore, there is an unmet

need to develop sensitive antibody and virus neutralization assays that are sufficiently robust for screening and monitoring large numbers of CoV-2 infected or convalescent subjects.

To overcome these experimental challenges, here we developed: 1) Highly sensitive bead-based fluorescent immunoassay for measuring CoV-2 specific antibody levels and isotypes, and 2) Robust CoV-2 Spike protein pseudovirus to measure NAb levels in COVID-19 patient plasma. We found striking differences in total antibody levels and neutralization titers between hospitalized or severe COVID-19 patients relative to outpatient or convalescent plasma donors, which were obtained with the purpose of transfer to and treatment of patients. Significant correlations between IgG and neutralization titers, age, duration of disease and NAbs to SARS were also observed. These assays and findings have important implications for assessing the breadth and depth of the humoral immune response during CoV-2 infection and for development of effective antibody-based therapies or vaccines.

Results

Development of SARS-CoV-2 specific antibody assay

Determining antibody responses in SARS-CoV-2 (CoV-2) infected subjects remains challenging, due to lack of sufficient dynamic range to determine precise antibody titers with antibody isotypes simultaneously. To overcome these obstacles, we developed a fluorescent bead-based immunoassay that takes advantage of the high dynamic range of fluorescent molecules using flow cytometry (Fig. 1a). In this assay, we immobilized biotinylated CoV-2 Spike protein receptor binding domain (RBD) or the Nucleoprotein (N) on streptavidin beads, to detect specific antibodies from patient plasma (Fig. 1a). Different antibody isotypes were measured using anti-Ig (IgG, IgA, IgM) specific secondary antibodies conjugated to a fluorescent tag (Fig. 1a). Using either anti-S-RBD antibody or soluble ACE2-Fc, we show very high sensitivity in detecting Spike protein

binding, down to picogram ranges (Fig. 1b). Similarly, S-RBD-specific antibodies were detectable in serial dilutions of plasma samples from CoV-2 PCR+ subjects at high specificity and sensitivity, up to 100,000-fold serial dilution of the plasma (Fig. 1c). We then used the titration curves from COVID-19 convalescent and healthy control plasma to normalize the area under the curve (AUC) values to quantitate the antibody levels (Supplementary Fig. 1a). Negative threshold values were set using healthy control AUC levels plus 3 times the standard deviations of the mean.

Using this assay, we screened COVID-19 patient or convalescent plasma samples (Table-1; n=87) for total S-RBD and Nucleocapsid specific IgG AUC values of COVID-19 positive subjects varied 3-logs from ~10^4 to ~10^7 (Fig. 2a). S-RBD specific IgM (33/41) and IgA (84/87) were also above the negative control threshold in most of the subjects (Fig. 2a). Furthermore, Nucleocapsid protein-specific IgG levels and S-RBD specific IgA positively correlated with S-RBD IgG antibodies (Supplementary Fig. 1b, c). Notably, IgG1 subclass antibody levels were comparable to total IgG levels whereas the other subtypes were relatively lower (Fig. 2b). There were significant differences in S-RBD or Nucleocapsid antibody levels between outpatient, hospitalized, and ICU/deceased subjects, with the highest levels observed in the most severe cases (Fig. 2c, d). Importantly, subjects who have recovered from COVID-19 and were also potential donors for convalescent plasma therapy (hereafter referred to as plasma donors), also had significantly lower antibody titers than hospitalized, intensive care unit (ICU) or deceased patients (Fig. 2c, d). In contrast to S-RBD IgG, S-RBD IgA levels were lower in ICU/deceased subjects compared to other hospitalized or outpatients (Fig. 2e). Overall, individual S-RBD and Nucleocapsid IgG levels appeared to correlate with their IgA, and IgG subclasses (IgG1-4) responses to S-RBD (Supplementary Fig. 1d). Subdividing the subjects by sex did not reveal any statistical difference in IgG levels at any of the disease stages, although hospitalized females in the non-ICU setting had significantly lower antibody levels than ICU/deceased patients, whereas the difference in males was not significant (Fig. 2f).

Table 1. Characteristics of CoV-2 infected and control subjects

		Outpatient (n=17)	Convalescent Plasma Donors (n=33)	Hospital (n=17)	ICU or Deceased (n=20)	Healthy Controls (n=20)
Sex	Male	3	18	7	9	9
	Female	14	15	10	11	11
Age	Mean (+-SEM)	41.9 (+-3.2)	45.5 (+-2.0)	62.8 (+-3.6)	67.8 (1.7)	45.9 (+-3.8)
	Median	39	48	63	69	44.5
Days between PCR/Blood	Mean (+-SEM)	34 (+-3.4)	65.4 (+-1.7)	20.5 (+-3.0)	24.5 (+-2.0)	N/A
	Median	39	66	28	24.5	N/A

Development of CoV-2 Spike protein pseudovirus

Next, we sought to develop a sensitive and high throughput CoV-2 neutralization assay by incorporating CoV-2 Spike protein onto lentiviruses to assess specific inhibition of these virus entry. To produce Spike protein pseudotyped lentiviral particles, we first ensured expression of the Spike protein on the cell membrane of transfected 293 cells, from which it would incorporate onto the lentiviruses. Human codon optimized CoV-2 Spike protein sequences with and without endoplasmic reticulum retention signal (ERRS), which would be predicted to be more efficiently expressed on the cell surface membranes, were cloned into an expression vector and transfected to 293 cells. To evaluate membrane expression of Spike protein, cells were stained with recombinant soluble ACE2-Fc fusion protein followed by a secondary staining with an anti-Fc antibody (Fig 3a). The percentage of Spike protein over-expressing cells was similar in the presence or absence of ERRS, but cells expressing Spike protein without ERRS showed a higher

geometric mean of expression (Fig. 3b). As such, we used Spike protein lacking the ERRS for lentiviral pseudotyping to ensure its higher incorporation into viral membranes.

We then co-transfected 293 cells with replication defective lentivectors encoding GFP or RFP reporter genes and the Spike protein encoding plasmid and harvested the supernatant at 24 hours, which was then used to infect cells expressing ACE2 (Fig. 3c). Bald particles were generated by transfecting lentivirus plasmids without any envelope and used as a negative control. Next, we tested the transduction efficiency of the viruses on wild type 293 cells, given they express low level endogenous ACE2 (Supplementary Fig. 2a, b). While we found clearly defined infection of 293 cells with Spike-protein pseudovirus compared to bald virions, infection rate determined as GFP or RFP expression was relatively low (Fig. 3d). We therefore generated human-ACE2 over-expressing 293 cells with a GFP reporter (ACE2-IRES-GFP) or fused to fluorescent mKO2 protein (ACE2-mKO2). ACE2 overexpression of ACE2-IRES-GFP or ACE2-mKO2 was confirmed by staining with CoV-2 Spike-protein fused with mouse Fc (mFc) and anti-mFc secondary antibody (Supplementary Fig. 2a, b). Indeed, these ACE2 overexpressing 293 cells (293-ACE2) were efficiently transduced with Spike protein pseudoviruses encoding either GFP or RFP (Fig. 3e). The efficiency of Spike-protein pseudovirus infection was comparable in ACE2-IRES-GFP or ACE2-mKO2 fusion protein (Fig. 3e), and therefore both were used in subsequent neutralization experiments. In addition, we also developed SARS Spike protein pseudotyped lentivirus, which similarly infected 293-ACE2 cells at almost 100% efficiency at higher virus supernatant volumes (Fig. 3f).

Neutralization of CoV-2 Spike protein pseudovirus with soluble ACE2, NAbs and COVID-19 plasma

We next investigated whether Spike protein pseudoviruses could be neutralized by soluble ACE2 (sACE) or Spike protein specific NAbs (Fig. 4a). For this experiment, Spike protein pseudotyped CoV-2 and SARS pseudovirus were pre-cultured with different concentrations of sACE2 or NAbs, then added to 293-ACE2 cells. Subsequently, infection was determined 3 days post-infection based on GFP or RFP expression as described above. sACE2 neutralized both CoV-2 and SARS pseudovirus infections in a dose dependent manner (Fig. 4b, c), although neutralization of CoV-2 was slightly better than that of SARS pseudoviruses (Fig. 4b, c, and Supplementary Fig. 3a). Furthermore, Spike-RBD specific NAbs neutralized CoV-2 pseudovirus entry much more efficiently than sACE2 but had no effect on SARS pseudovirus (Fig. 4c). We also observed measurable differences in the neutralizing activity of three different Nabs and 2 different soluble Ace2 proteins from two different sources (Fig. 4d), showing the utility of this assay for such screening. Taken together, these experiments demonstrate that the combination of pseudotyped viruses and 293-ACE2 cells can be used to generate highly sensitive CoV-2 and SARS neutralization assays.

Using this approach, we then tested neutralization titers from COVID-19 patients or seropositive donors with serial dilution of their plasma. Accordingly, plasma samples were incubated with Spike pseudovirus and added to 293-ACE2 cells in 3-fold serial dilutions and infection was determined as described in Figure 4. Healthy control plasma samples were used as negative controls whereas anti-S-RBD NAb served as a positive control (Fig. 5a). None of the control plasma (n=20, 1 shown in Fig. 5a) tested showed any neutralization activity, whereas patient plasma efficiently neutralized the virus to 10,000-fold serial dilution (Fig. 5a). The 50% neutralization titer (NT50), was determined using the half-maximal inhibitory concentration values of plasma samples, normalized to control infections, from their serial dilutions. Importantly, the NT50 values of the subjects were much higher in hospitalized patients than outpatients (Fig. 5b). NT50 values for hospitalized and ICU/deceased subjects were also up to 1000-fold higher than

convalescent plasma donors (Fig. 5b). Hospitalized males and females, separately, also remained higher in their NT50 levels and no difference was observed within each group (Fig. 5c).

We also tested whether CoV-2 PCR+ plasma could neutralize the SARS pseudovirus. 14 plasma samples from hospitalized group were tested for their ability to neutralize CoV-2 and SARS pseudoviruses. Remarkably, some of the plasma samples also neutralized SARS pseudovirus, although less efficiently than CoV-2 pseudovirus (Fig. 5d). Interestingly, NT50 levels of plasma samples for CoV-2 and SARS were positively correlated (Fig. 5e, Supplementary Fig. 3b)

Correlations of CoV-2 neutralization, antibody levels and COVID-19 subject characteristics

To better understand the associations between patient characteristics and the humoral immune response in COVID-19, we next determined correlations between antibody AUC levels, NT50 values and demographics of the study subjects. First, we assessed the correlation between NT50 values with S-RBD or Nucleocapsid antibody titers or their subclasses. All Igs including S-RBD IgG (r_s = 0.85), Nucleocapsid IgG (r_s = 0.72), S-RBD IgA (r_s = 0.69) and S-RBD IgM (r_s = 0.47) showed high correlation with NT50 values of each subject (Fig. 6a). Among Ig subclasses specific to S-RBD; IgG1 (r_s = 0.82), IgG3 (r_s = 0.71) and IgG2 (r_s = 0.67) and to less degree with IgG4 (r_s = 0.52) also correlated with NT50 values (Fig. 6b). Total S-RBD IgG, also correlated in similar fashion with other IgG isotypes, with IgG1 showing the highest positive correlation (r_s = 0.97) (Supplementary Fig. 4).

Next, we correlated the antibody AUC levels and NT50 values of the subjects with their age. Subjects had significantly higher S-RBD IgG (r_s = 0.61), Nucleocapsid IgG (r_s = 0.46), S-RBD IgA (r_s = 0.5) and NT50 (r_s = 0.56) values, with increased age (Fig. 6c). We also explored the

relationship between the number of days between PCR test result and blood draw correlated with antibody levels or NT50 values excluding the subjects that had less than 15 days or fewer between those dates to ensure the antibody levels had already reached their peak. Of note, there was a significant negative correlation between the number of days and the IgG or IgA to S-RBD, anti-nucleocapsid IgG or the NT50 values (r_s = -0.67) (Fig. 6d), suggesting a potential decline in antibody titers over time.

Discussion

The COVID-19 pandemic is continuing to spread globally unabated, including within the United States. There is an urgent need to better understand the immune response to the virus so that effective immune-based treatments and vaccines can be developed[16,17]. Neutralization of the virus by antibodies (NAbs) is one of the goals to achieve protection against CoV-2[18]. Despite rapid development of many serological tests, important questions about the quality and quantity of seroprevalence in individuals remains still unclear[19,20]. Here, we developed highly sensitive and specific humoral assays that measure both the magnitude and neutralization capacity of antibody responses in COVID-19 patients. Every SARS-CoV-2 infected subject we tested (n=87) had detectable antibodies and all subjects except one exhibited neutralization; both of these qualities were completely absent in non-infected controls. However, there was a profound difference in antibody and neutralization titers among subjects, ranging in more than 1000-fold differences. Furthermore, we found that some COVID-19 patients with high antibody titers also had neutralizing antibodies for SARS, suggesting a high degree of cross-reactivity between these two virus Spike proteins.

One of our key findings was clustering of antibody responses based on severity of the disease; as hospitalized patients showed much higher antibody levels and neutralization capacity than

outpatient subjects or convalescent plasma donors. This finding is consistent with recent reports suggesting that patients with more severe disease contain relatively higher antibodies for SARS-CoV-2 infection[2,21,22]. Interestingly, most of the convalescent plasma donors had much lower level of neutralizing antibodies (by at least an order of magnitude) than hospitalized patients, who would be the suitable recipients for such plasma transfer therapy. This finding raises the question of whether convalescent plasma transfers may actually provide benefit to severe COVID-19 patients by providing neutralizing antibodies. It may perhaps be more beneficial to identify donors with much higher neutralizing antibody titers for the plasma donation. As such, our findings point to the importance of having access to assays that have a large dynamic range to detect antibody responses in COVID-19 patients or seropositive individuals. This neutralization assay also revealed differences in commercial antibodies to CoV-2 in their capacity to block virus entry, and as such can be used for rapid identification or generation of synthetic NAbs. In addition to measuring neutralization titers, the pseudoviruses can be used to probe cells that have the potential to be infected with CoV-2, given lentiviruses can infect most cell types and does not require cell division to integrate into the genome. This infection assay may also be used to screen small molecules that may impact virus cell entry.

Along with CoV-2, we also developed a pseudotyped lentivirus with SARS Spike protein, which was equally efficient at infecting ACE2 overexpressing cells. This finding is consistent with results that CoV-2 Spike protein in complex binding with human ACE2 (hACE2) is similar overall to that observed for SARS[23]. There was however slightly better neutralization of CoV-2 cell entry than SARS with soluble ACE2, which could be due to key residue substitutions in CoV-2 creating a slightly stronger interaction and thus higher affinity for receptor binding than SARS Spike protein[23]. Accordingly, we also tested the ability of hospitalized COVID-19 patient plasma for SARS neutralizing capacity and found significant SARS-specific neutralization in COVID-19

patients who also had high neutralization activity for CoV-2. Indeed, there was a very high level of correlation between titers of both viruses from the same donors (Fig. 5e). Given that the two viruses share ~75% identical amino acids in their Spike proteins and there are conserved epitopes between them[24], it is conceivable that some of the CoV-2 NAbs have cross-neutralizing activity[25,26]. This discrepancy could be due to differences in sensitivity in our respective assays, since the SARS neutralization was about an order of magnitude lower than the CoV-2 entry block. It is noteworthy that a recent study showed a NAb developed for SARS was highly effective at neutralizing CoV-2[27].

The use of flow cytometry bead based fluorescent system that detects Spike or Nucleocapsid protein bound antibodies provides a high-throughput assay with a very high dynamic range and sensitivity, as it could detect antibodies from some subjects at up to a million-fold dilution of the plasma. This assay is also scalable and can also be easily adaptable to other viral antigens. Using a flow cytometry platform is also important in that the assay can further be developed in a single panel to identify all antibody isotypes simultaneously and to complement flow cytometric immune phenotyping of COVID-19 patients. The high sensitivity and specificity of our assay has allowed us to correlate the Spike protein RBD-specific antibody levels with neutralization titers, which showed very high concordance, thus can be utilized as a proxy for neutralization in a clinical setting. Furthemore, bead-based immunoassay can also be further developed to screen for antibodies reacting to other CoV-2 antigens simultaneously and can be useful to identify antibodies that cross-react between different species of coronavirus proteins.

Determining other isotypes such as IgA and IgG subclasses may also help in future mechanistic studies. It is clear that the dominant antibody response in almost all donors was IgG1, but some also show high IgA and IgG2-4, at varying levels. In particular, it is interesting to note that, in contrast to Spike protein-specific IgG, IgA antibody levels are not higher between hospitalized

and outpatients, and in fact are strikingly lower in ICU/deceased patients (Fig. 2e). However, another study showed IgA antibodies, but not IgG, increased in severe patients[28]. While the significance of these findings or discrepancy are not yet clear, it is conceivable that given the importance of IgA antibodies in providing immunity on mucosal surfaces within the respiratory system, CoV-2 RBD-spike protein specific IgA levels may also play an important role in upper and lower respiratory system, or perhaps also in gut, of COVID-19 patients[29,30].

There are also several potential practical implications to our findings. First, the patient population with the highest risk factors for severe outcomes from infection such as age and co-morbid conditions had the highest antibody titers as well as neutralization of the virus. This is also the case for those patients who had lethal disease. It is therefore possible that surviving COVID-19 may require non-antibody dependent factors or that producing too much antibody may even have deleterious effects. Potential antibody-dependent enhancement phenomenon by triggering Fc receptors on macrophages[31]. In this regard, it is interesting to note that a bruton tyrosine kinase (BTK) inhibitor, that targets Fc-receptor signaling in macrophages, is being tested in a randomized clinical trial [32]. Another interesting observation is that further out from the infection, there appears to be less antibody response. Although it will be important to follow the same individual subject convalescent plasma over time to better assess this finding, our data point towards a relatively short-lived antibody response to COVID-19. Thus, understanding the mechanism of survival from COVID-19 and immune response dynamics will be critical, in better prediction of outcomes as well as assaying for a protective response to potential vaccines.

In conclusion, the assays developed herein can have a utility in uncovering dynamic changes in the antibody levels in SARS-CoV-2 infected subjects over time, in responses to vaccines, and as potential clinical determinants for plasma or antibody therapies for COVID-19 patients.

Materials and Methods

Participants

COVID-19 subjects (n=87) were recruited at Suny downstate medical center, New York, NY, Cedars Sinai, Los Angeles, CA, or the University of Connecticut, School of Medicine, Farmington CT following testing and/or admission for COVID-19 infection. Written informed consent obtained from all participants in this study and was approved by the following IRBs: 1) IRB# SUNY:269846. The patients were recruited at SUNY Downstate, NY and processed and biobanked at Amerimmune, Fairfax VA; 2) IRB# STUDY00000640 Convalescent plasma was collected at Cedars Sinai Medical Center according to FDA protocol (https://www.fda.gov/vaccines-blood-biologics/investigational-new-drug-ind-or-device-exemption-ide-process-cber/recommendations-investigational-covid-19-convalescent-plasma#Collection%20of%20COVID-19). The source of the convalescent plasma was volunteer blood donors who were recovered from COVID-19. Donors met routine blood donor eligibility requirements established by the FDA and had a prior SARS-CoV-2 infection documented by a laboratory test for the virus during illness, or antibodies to the virus after recovery of suspected disease. All donors were least 28 days from either resolution of COVID-19 symptoms or diagnosis, whichever was longer; 3) IRB# 20-186-1. UConn Healthcare workers who tested positive for the virus by PCR were recruited and samples banked for future testing. 4) IRB#: 17-JGM-13-JGM or 16-JGM-06-JGM. De-identified control subjects (n=20) used were previously frozen (more than a year ago) samples obtained from healthy controls or determined to be CoV-2 PCR negative (IRB SUNY:269846). All antibody assays were performed at the Jackson Laboratory for genomic Medicine, Farmington, CT. Subject characteristics are shown in Table 1. All plasma samples were aliquoted and stored at -80°C. Prior to experiments, aliquots of plasma samples were heat-inactivated at 56°C for 30 minutes.

Over-expression of SARS-CoV-2 Spike protein and cell culture

Human codon optimized CoV-2 Spike protein sequence was synthesized by MolecularCloud (MC_0101081) and cloned into pCMV vector with and without the last 19 amino acids which contain an endoplasmic reticulum retention signal. HEK-293T cells (ATCC; mycoplasma-free low passage stock) were transfected with the expression plasmids using Lipofectamine 3000 (Invitrogen) according to the manufacturer's protocol as previously described[33]. The cells were cultred in complete RPMI 1640 medium (RPMI 1640 supplemented with 10% FBS; Atlanta Biologicals, Lawrenceville, GA), 8% GlutaMAX (Life Technologies), 8% sodium pyruvate, 8% MEM vitamins, 8% MEM nonessential amino acid, and 1% penicillin/streptomycin (all from Corning Cellgro) for 72 hours, collected using %0.05 Trypsin-0.53 mM EDTA (Corning Cellgro) and stained with Biotinylated Human ACE2 / ACEH Protein, Fc,Avitag (Acro Biosystems) then stained with APC anti-human IgG Fc Antibody clone HP6017 (Biolegend). Samples were acquired on a BD FACSymphony A5 analyzer and data were analyzed using FlowJo (Tree Star).

Pseudotyped lentivirus production and titer measurement

Lentivector plasmids containing RFP or GFP reporter gene were co-transfected with either SARS-CoV-2 Spike protein or SARS Spike protein plasmids into HEK-293T cells using Lipofectamine TM 3000 (Invitrogen) according to the manufacturer's protocol. Viral supernatants were collected 24-48 hours post-transfection and filtered through a 0.45 μm syringe filter (Millipore) to remove cellular debris. Lentivirus supernatant stocks were aliquoted and stored at −80°C. To measure viral titers, virus preps were serially diluted on ACE2 over-expressing 293 cells. 72 hours after infection, GFP or RFP positive cells were counted using flow cytometry and the number of cells transduced with virus supernatant was calculated as infectious units/per ml.

Generating human ACE2 over-expressing cells

Wildtype ACE2 sequence was obtained from Ensembl Gene Browser (Transcript ID: ENST00000252519.8) and codon optimized with SnapGene by removing restriction enzyme recognition sites necessary for subsequent molecular cloning steps, preserving the amino acid sequence. mKO2 (monomeric Kusabira-Orange-2[34]), obtained from Addgene (#54625)[35], sequence was added onto the C terminal end of ACE2 before the stop codon with a small linker peptide (ccggtcgccacc) encoding the amino acids PVAT. The fusion constructs were synthesized via GenScript and cloned into a lentiviral vector lacking a fluorescent reporter. The full length human ACE2 sequence without fusion fluorescent proteins was amplified from the ACE2-mKO2 fusion a construct using 5'-ACGACGGCGGCCGCATGTCAAGCTCTTCCTGGC-3' and 5'-ACGACGGAATTCTTAAAAGGAGGTCTGAACATCATCAG-3' primers, generating a stop codon at the C-terminus, and then cloned into a lentiviral vector encoding GFP reporter separated from multiple cloning site via an internal ribosome entry site (IRES) sequence. To determine virus titers, HEK-293T cells were transduced with full length ACE2-IRES-GFP, ACE2-mKO2 fusion construct lentiviruses and analyzed via flow cytometry for their reporter gene expression 72 hours after infection. WT and ACE2 over-expressing HEK-293T were also stained with SARS-CoV-2 S1 protein, Mouse IgG2a Fc Tag (Acro Biosystems) followed with APC Goat anti-mouse IgG2a Fc Antibody (Invitrogen). Samples were acquired on a BD FACSymphony A5 analyzer and data were analyzed using FlowJo (BD Biosciences).

SARS-CoV-2 antibody detection using Flow immunoassay

To screen for antibodies binding to CoV-2 proteins, The DevScreen SAv Bead kit (Essen BioScience, MI) was used. Biotinylated 2019-nCoV (COVID-19) Spike protein RBD, His,Avitag and Biotinylated CoV-2 (COVID-19) Nucleocapsid protein, His,Avitag (Acro Biosystems, DE) were coated to SAv Beads according to manufacturer's instructions. Confirmation of successful bead

conjugation was determined by staining with anti-His Tag (Biolegend) and flow cytometry analysis. S-RBD and N conjugated beads were then used as capture beads in flow immunoassay where they were incubated with anti-S-RBD human IgG positive control (provided in Genscript CoV-2 Spike S1-RBD IgG & IgM ELISA Detection Kit as positive control), recombinant Human ACE2-Fc (Acro Biosystems) or plasma and serum samples for 1 hour at room temperature. Plasma samples were assayed at a 1:100 starting dilution and 3 additional 10-fold serial dilutions. Anti-S-RBD antibody and ACE2-Fc was tested both at 5 μg/mL starting concentration and in additional 5-fold serial dilutions. Detection reagent was prepared using Phycoerythrin-conjugated anti-human IgG Fc clone HP6017, anti-human IgM clone MHM-88 (Biolegend), anti-human IgA clone IS11-8E10, anti-human IgG1 clone IS11-12E4.23.20 (Miltenyi Biotec), anti-human IgG2 Fc clone HP6002, anti-human IgG3 Hinge clone HP6050 and anti-human IgG4 pFc clone HP6023 (Southern Biotech), added to the wells and incubated for another hour at room temperature. Plates were then washed twice with PBS and analyzed by flow cytometry using iQue Screener Plus (IntelliCyt, MI). Flow cytometry data were analyzed using FlowJo (BD biosciences). Geometric means of PE fluorescence in different titrations were used to generate the titration curve and 20 healthy control plasma were used to normalize the area under the curve (AUC). Statistical analyses were performed using GraphPad Prism 8.0 software (GraphPad Software).

Pseudotype virus neutralization assay

Three-fold serially diluted monoclonal antibodies including anti-SARS-CoV-2 Neutralizing human IgG1 Antibody from Acro Biosystems, NAb#3 (Fig 4D), Genscript clone ID 6D11F2, NAb#2 (Fig 4D) and Genscript clone ID 10G6H5, NAb#1 (Fig 4D), recombinant human ACE2-Fc (Acro Biosystems, sACE2#1 and Genscript, sACE2#2 (Fig 4D)) or plasma from COVID-19 convalescent individuals and healthy donors were incubated with RFP-encoding CoV-2 or GFP-encoding SARS pseudotyped virus for 1 hour at 37°C degrees. The mixture was subsequently

incubated with 293-ACE2 cells for 72h hours after which cells were collected, washed with FACS buffer (1xPBS+2% FBS) and analyzed by flow cytometry using BD FACSymphony A5 analyzer. Percent infection obtained was normalized samples derived from cells infected with CoV-2 or SARS pseudotyped virus in the absence of plasma, ACE2-Fc or monoclonal antibodies. The half-maximal inhibitory concentration for plasma (NT50), ACE2-Fc or monoclonal antibodies (IC50) was determined using 4-parameter nonlinear regression (GraphPad Prism 8.0).

Data availability

The source data for the Figures along with the Supplementary Figures presented in this paper are available upon request.

Acknowledgements

The research in this study was supported by National Institute of Health (NIH) grants R01AI121920, U54 NS105539 and U19 AI142733 to D.U. We thank Tina Vaziri for critical reading.

Author contributions

M.D., L.K. and D.U. conceived, designed the experiments. M.D., L.K., L.P., M.Y. and R.H. carried out the experiments. B.T.L. designed the clinical research study on UConn Healthcare workers and M.K. recruited participants and executed clinical protocols. R.G. and O.A designed the clinical research study at Suny state medical center, Z.B., M.B, P.C and K.L, recruited, processed, coordinated and executed the clinical protocols. M.A., E.K., N.M. and C.H, designed, recruited and stored convalescent plasma samples at Cedars Sinai hospital. M.D., L.K, C.L.G. and D.U. analyzed the data, performed statistics, drew illustrations and prepared the figures. M.D. and D.U. wrote the manuscript.

References

1 Hoffmann, M. *et al.* SARS-CoV-2 Cell Entry Depends on ACE2 and TMPRSS2 and Is Blocked by a Clinically Proven Protease Inhibitor. *Cell* **181**, 271-280 e278, doi:10.1016/j.cell.2020.02.052 (2020).

2 Robbiani, D. F. *et al.* Convergent antibody responses to SARS-CoV-2 in convalescent individuals. *Nature*, doi:10.1038/s41586-020-2456-9 (2020).

3 Rogers, T. F. *et al.* Isolation of potent SARS-CoV-2 neutralizing antibodies and protection from disease in a small animal model. *Science*, doi:10.1126/science.abc7520 (2020).

4 Wu, Y. *et al.* Identification of Human Single-Domain Antibodies against SARS-CoV-2. *Cell Host Microbe* **27**, 891-898 e895, doi:10.1016/j.chom.2020.04.023 (2020).

5 Wang, C. *et al.* A human monoclonal antibody blocking SARS-CoV-2 infection. *Nat Commun* **11**, 2251, doi:10.1038/s41467-020-16256-y (2020).

6 Seydoux, E. *et al.* Analysis of a SARS-CoV-2-Infected Individual Reveals Development of Potent Neutralizing Antibodies with Limited Somatic Mutation. *Immunity*, doi:10.1016/j.immuni.2020.06.001 (2020).

7 Duan, K. *et al.* Effectiveness of convalescent plasma therapy in severe COVID-19 patients. *Proc Natl Acad Sci U S A* **117**, 9490-9496, doi:10.1073/pnas.2004168117 (2020).

8 Barone, P. & DeSimone, R. A. Convalescent plasma to treat coronavirus disease 2019 (COVID-19): considerations for clinical trial design. *Transfusion* **60**, 1123-1127, doi:10.1111/trf.15843 (2020).

9 Bloch, E. M. *et al.* Deployment of convalescent plasma for the prevention and treatment of COVID-19. *J Clin Invest* **130**, 2757-2765, doi:10.1172/JCI138745 (2020).

10 Chen, B. & Xia, R. Early experience with convalescent plasma as immunotherapy for COVID-19 in China: Knowns and unknowns. *Vox Sang*, doi:10.1111/vox.12968 (2020).

11 Lisboa Bastos, M. *et al.* Diagnostic accuracy of serological tests for covid-19: systematic review and meta-analysis. *Bmj*, doi:10.1136/bmj.m2516 (2020).

12 Huang, A. T. *et al.* A systematic review of antibody mediated immunity to coronaviruses: antibody kinetics, correlates of protection, and association of antibody responses with severity of disease. *medRxiv*, doi:10.1101/2020.04.14.20065771 (2020).

13 Hicks, J. *et al.* Serologic cross-reactivity of SARS-CoV-2 with endemic and seasonal Betacoronaviruses. *medRxiv*, doi:10.1101/2020.06.22.20137695 (2020).

14 Nagappa, B. & Marimuthu, Y. Seroconversion rate and diagnostic accuracy of serological tests for COVID-19. *Clin Infect Dis*, doi:10.1093/cid/ciaa676 (2020).

15 Che, X. Y. *et al.* Antigenic cross-reactivity between severe acute respiratory syndrome-associated coronavirus and human coronaviruses 229E and OC43. *J Infect Dis* **191**, 2033-2037, doi:10.1086/430355 (2005).

16 St John, A. L. & Rathore, A. P. S. Early Insights into Immune Responses during COVID-19. *J Immunol*, doi:10.4049/jimmunol.2000526 (2020).

17 Yazdanpanah, F., Hamblin, M. R. & Rezaei, N. The immune system and COVID-19: Friend or foe? *Life Sci* **256**, 117900, doi:10.1016/j.lfs.2020.117900 (2020).

18 Tong, P. B., Lin, L. Y. & Tran, T. H. Coronaviruses pandemics: Can neutralizing antibodies help? *Life Sci* **255**, 117836, doi:10.1016/j.lfs.2020.117836 (2020).

19 Deeks, J. J. *et al.* Antibody tests for identification of current and past infection with SARS-CoV-2. *Cochrane Database Syst Rev* **6**, CD013652, doi:10.1002/14651858.CD013652 (2020).

20 Siracusano, G., Pastori, C. & Lopalco, L. Humoral Immune Responses in COVID-19 Patients: A Window on the State of the Art. *Front Immunol* **11**, 1049, doi:10.3389/fimmu.2020.01049 (2020).

21 Ma, H. *et al.* Serum IgA, IgM, and IgG responses in COVID-19. *Cell Mol Immunol*, doi:10.1038/s41423-020-0474-z (2020).

22 Zhao, J. *et al.* Antibody responses to SARS-CoV-2 in patients of novel coronavirus disease 2019. *Clin Infect Dis*, doi:10.1093/cid/ciaa344 (2020).

23 Wang, Q. *et al.* Structural and Functional Basis of SARS-CoV-2 Entry by Using Human ACE2. *Cell* **181**, 894-904 e899, doi:10.1016/j.cell.2020.03.045 (2020).

24 Walls, A. C. *et al.* Structure, Function, and Antigenicity of the SARS-CoV-2 Spike Glycoprotein. *Cell* **181**, 281-292 e286, doi:10.1016/j.cell.2020.02.058 (2020).

25 Ou, X. *et al.* Characterization of spike glycoprotein of SARS-CoV-2 on virus entry and its immune cross-reactivity with SARS-CoV. *Nat Commun* **11**, 1620, doi:10.1038/s41467-020-15562-9 (2020).

26 Lv, H. *et al.* Cross-reactive antibody response between SARS-CoV-2 and SARS-CoV infections. *bioRxiv*, doi:10.1101/2020.03.15.993097 (2020).

27 Pinto, D. *et al.* Cross-neutralization of SARS-CoV-2 by a human monoclonal SARS-CoV antibody. *Nature*, doi:10.1038/s41586-020-2349-y (2020).

28 Yu, H. Q. *et al.* Distinct features of SARS-CoV-2-specific IgA response in COVID-19 patients. *Eur Respir J*, doi:10.1183/13993003.01526-2020 (2020).

29 Padoan, A. *et al.* IgA-Ab response to spike glycoprotein of SARS-CoV-2 in patients with COVID-19: A longitudinal study. *Clin Chim Acta* **507**, 164-166, doi:10.1016/j.cca.2020.04.026 (2020).

30 Ejemel, M. *et al.* IgA MAb blocks SARS-CoV-2 Spike-ACE2 interaction providing mucosal immunity. *bioRxiv*, doi:10.1101/2020.05.15.096719 (2020).

31 Ulrich, H., Pillat, M. M. & Tarnok, A. Dengue Fever, COVID-19 (SARS-CoV-2), and Antibody-Dependent Enhancement (ADE): A Perspective. *Cytometry A*, doi:10.1002/cyto.a.24047 (2020).

32 Roschewski, M. *et al.* Inhibition of Bruton tyrosine kinase in patients with severe COVID-19. *Sci Immunol* **5**, doi:10.1126/sciimmunol.abd0110 (2020).

33 Chen, X. *et al.* Functional Interrogation of Primary Human T Cells via CRISPR Genetic Editing. *J Immunol* **201**, 1586-1598, doi:10.4049/jimmunol.1701616 (2018).

34 Karasawa, S., Araki, T., Nagai, T., Mizuno, H. & Miyawaki, A. Cyan-emitting and orange-emitting fluorescent proteins as a donor/acceptor pair for fluorescence resonance energy transfer. *Biochem J* **381**, 307-312, doi:10.1042/BJ20040321 (2004).

35 Sakaue-Sawano, A. *et al.* Visualizing spatiotemporal dynamics of multicellular cell-cycle progression. *Cell* **132**, 487-498, doi:10.1016/j.cell.2007.12.033 (2008).

Figure 1

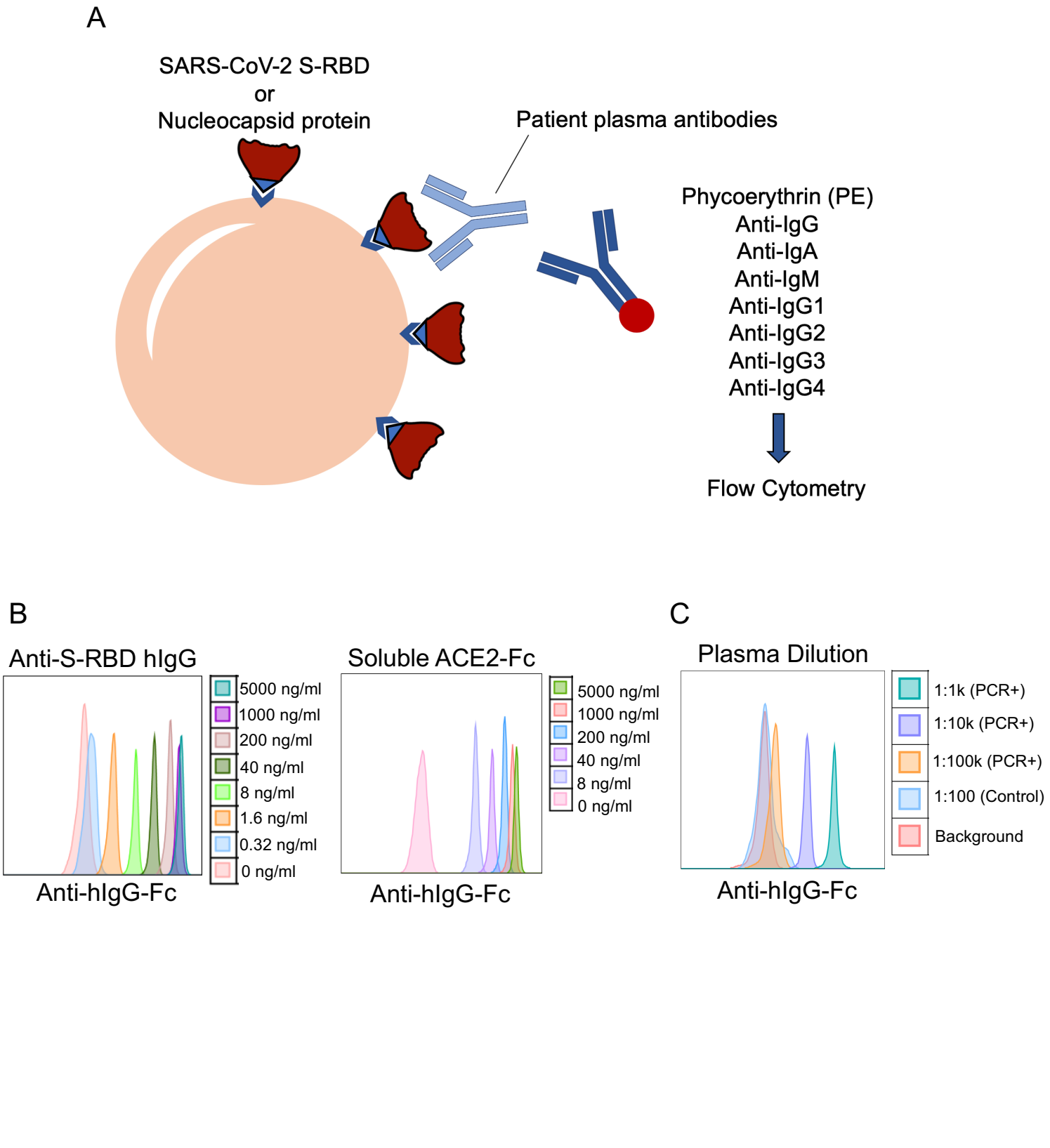

Fig. 1: SARS-CoV-2 specific antibody detection assay.

a. Illustration of antibody detection assay. Biotinylated S-RBD or Nucleocapsid proteins are captured by streptavidin coated beads, then incubated with plasma samples and stained with PE conjugated anti-IgG, IgA, IgM, IgG1, IgG2, IgG3, IgG4 antibodies. Fluorescence intensity analyzed by flow cytometry. **b.** Histogram overlays demonstrating the detection of anti-S-RBD human IgG antibody (left) and soluble ACE2-Fc (right) as positive controls for plasma antibody assay. **c**. Representative patient plasma titration. Healthy control plasma at 1:100 dilution was used as a negative control**.** Serial dilutions used were used in the flow cytometry overlay.

Figure 2

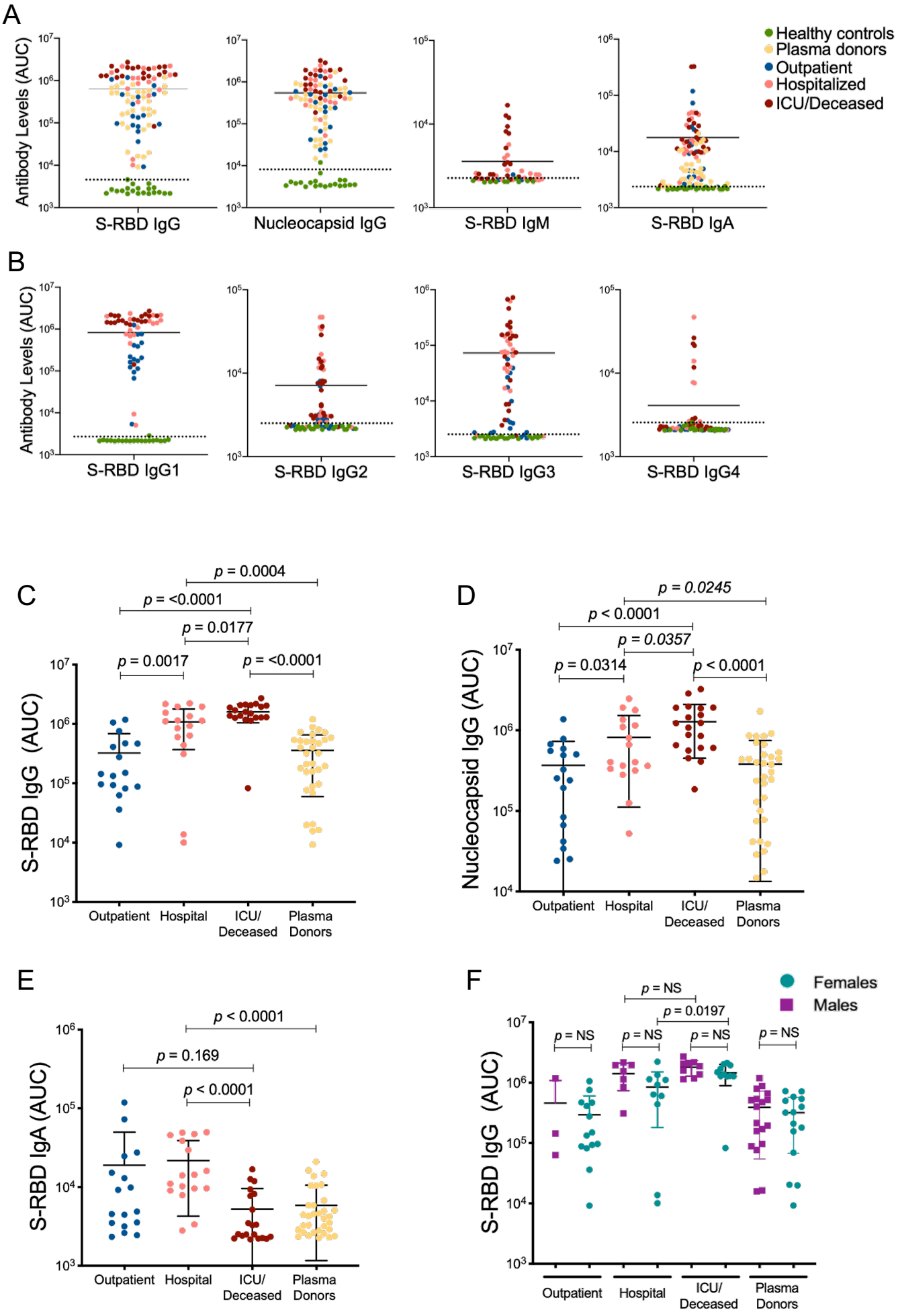

Fig. 2: CoV-2 specific antibody detection in COVID-19 and convalescent plasma samples.

a. Measurement of Spike protein and Nucleocapsid protein specific IgG and Spike protein specific IgM and IgA antibodies as described in Figure 1. Area under the curve (AUC) values of plasma antibodies were calculated from reciprocal dilution curves in antibody detection assay. Dotted lines indicate the negative threshold calculated by adding 3 standard deviations to the mean AUC values of healthy controls' plasma. **b.** S-RBD specific IgG subclass AUC levels. **c.** S-RBD IgG AUC values of subject plasma grouped by outpatient, hospitalized, ICU or deceased and plasma donors. **d.** Nucleocapsid protein IgG AUC values of subject plasma grouped by outpatient, hospitalized, ICU or deceased and convalescent plasma donors. **e.** S-RBD IgA AUC values of subject plasma grouped by outpatient, hospitalized, ICU or deceased and plasma donors. **f.** S-RBD IgG AUC values of severity groups and plasma donors subdivided into males and females. Statistical significances were determined using two-tailed Mann-Whitney U test.

Figure 3

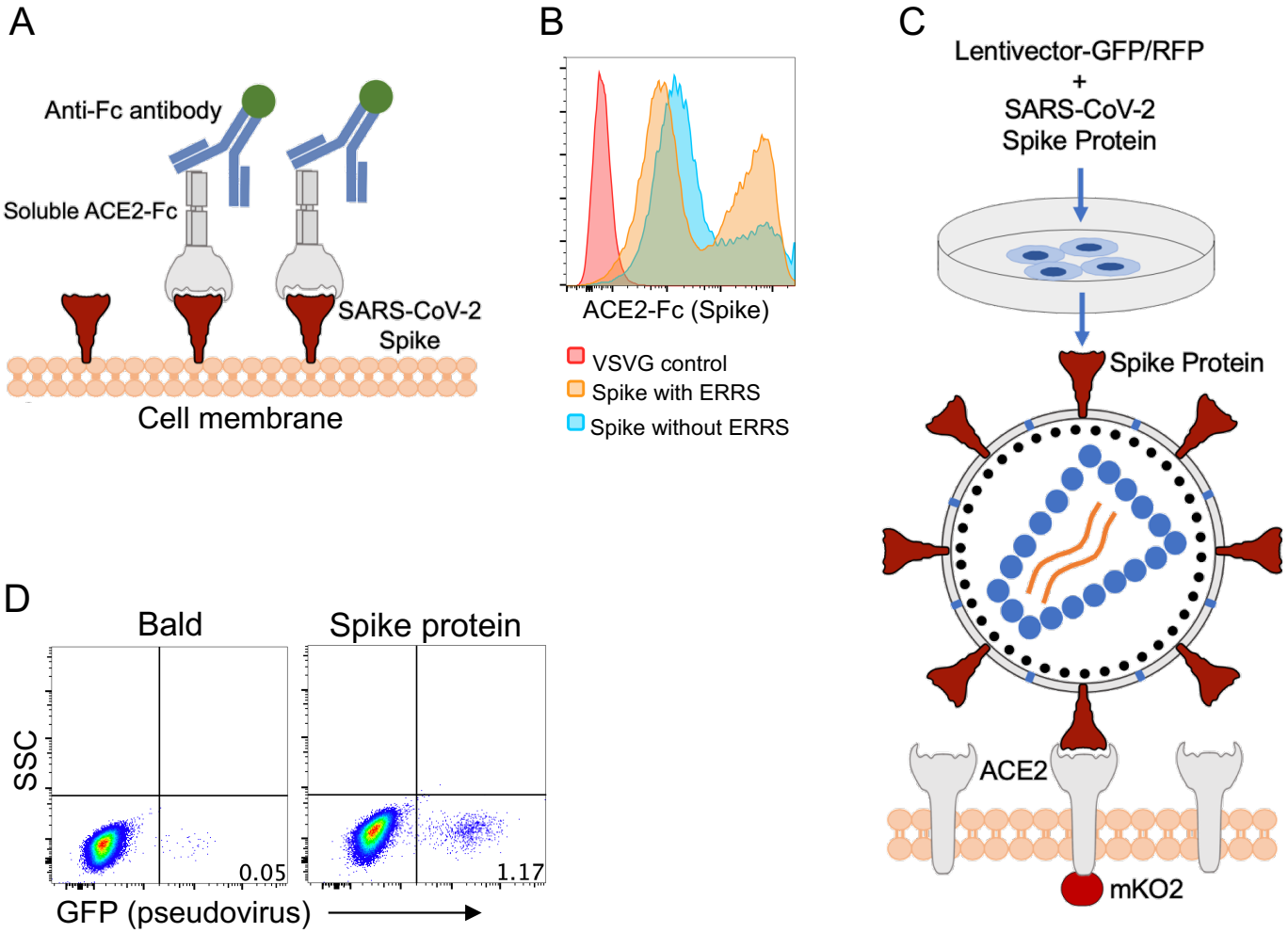

Fig. 3: Development of CoV-2 and SARS Spike protein pseudotyped lentiviruses.

a. Schematic illustration of Spike protein expression on the cell surface and soluble ACE2-Fc staining followed by an anti-Fc antibody staining. **b.** 293 cells transfected with Spike protein with or without endoplasmic reticulum retention signal (ERRS) and VSV-G as negative control. The cells were stained with ACE2-Fc and anti-Fc-APC secondary antibody, flow cytometry data overlays are shown. **c.** Schematic representation of the generation of Spike protein pseudovirus and the interaction with ACE2-expressing host cells. A lentivector plasmid and a Spike protein over-expressing envelope plasmid are used to co-transfect 293 cells to generate Spike pseudovirus that in turn infect engineered cells over-expressing wild type ACE2 or ACE2 fused to mKO2. **d.** Infection of wild type 293 cells with either bald lentiviruses generated without envelope plasmid or Spike protein pseudovirus. **e.** Infection of 293-ACE2 cells with bald and Spike lentiviruses. GFP and mKO2 markers are used to determine ACE2 over-expressing cells in ACE2-IRES-GFP and ACE2-mKO2, respectively. **f.** The titration of CoV-2 and SARS Spike protein pseudoviruses encoding RFP. ACE2-IRES-GFP expressing 293 cells were incubated with 3-fold serial dilutions of virus supernatant and analyzed for RFP expression by flow cytometry on day 3 post-infection. Percent infection is % RFP+ cells after gating on GFP+ cells (i.e. ACE2+).

Figure 4

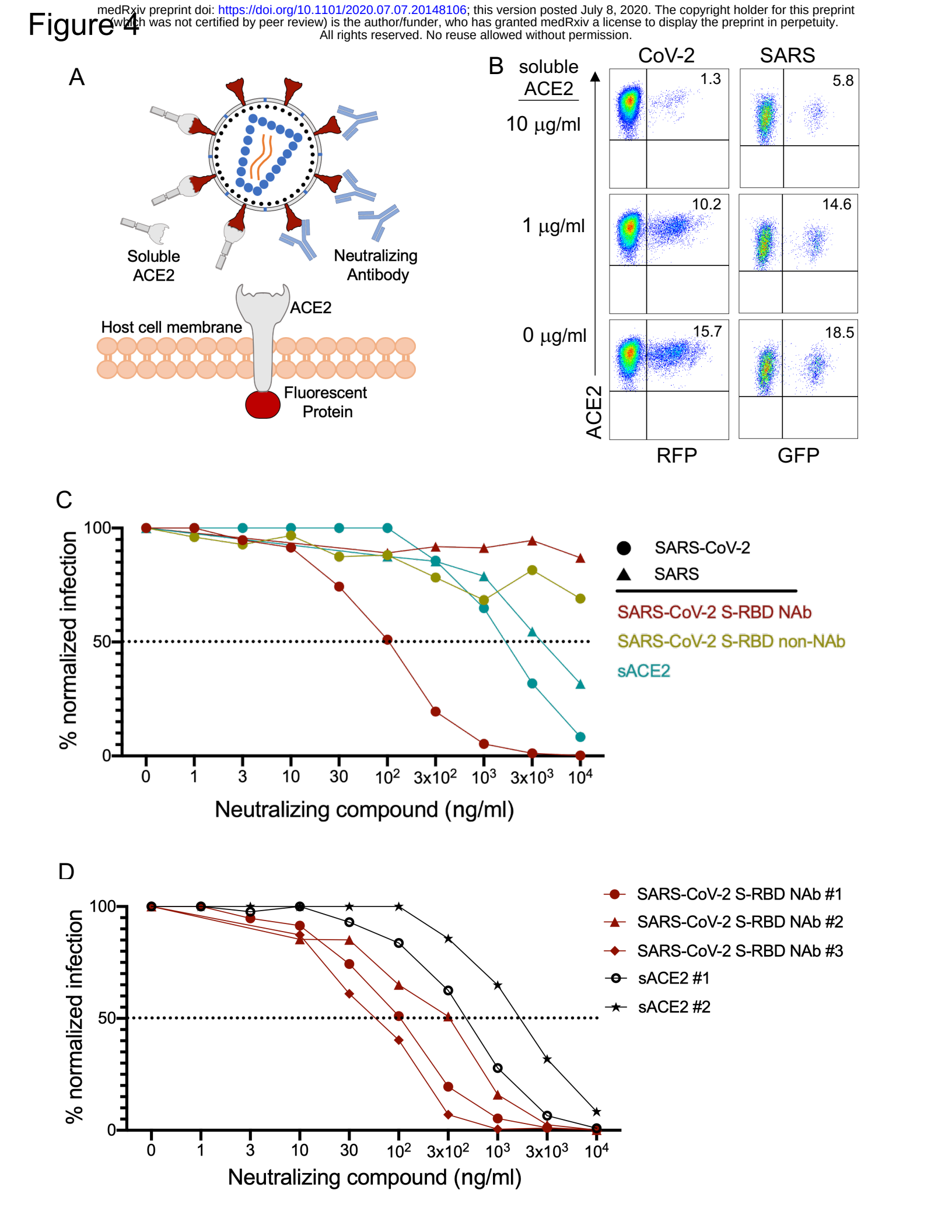

Fig. 4: Neutralization of CoV-2 and SARS pseudoviruses with soluble ACE2 and NAbs

a. Illustration of Spike protein pseudovirus blocked by soluble ACE2 or neutralizing antibodies. **b.** CoV-2 and SARS pseudovirus neutralization with soluble ACE2. CoV-2 RFP and SARS GFP pseudoviruses were preincubated with soluble ACE2 for 1 hour and added to 293 cells expressing ACE2-IRES-GFP or ACE2-mKO2 fusion respectively. **c.** Neutralization of CoV-2 and SARS with S-RBD specific antibodies and soluble ACE2 (sACE2). Viruses were pre-incubated with antibodies or soluble ACE2 for 1 hour at the concentrations shown and subsequently added to target cells. Expression of RFP was determined at day 3 post-infection. Infection percentages were normalized to negative controls. **d.** Neutralization of CoV-2 pseudoviruses using 3 different S-RBD NAbs and soluble ACE2 (sACE2) protein from two different sources. Representative experiment out of two is shown.

Figure 5

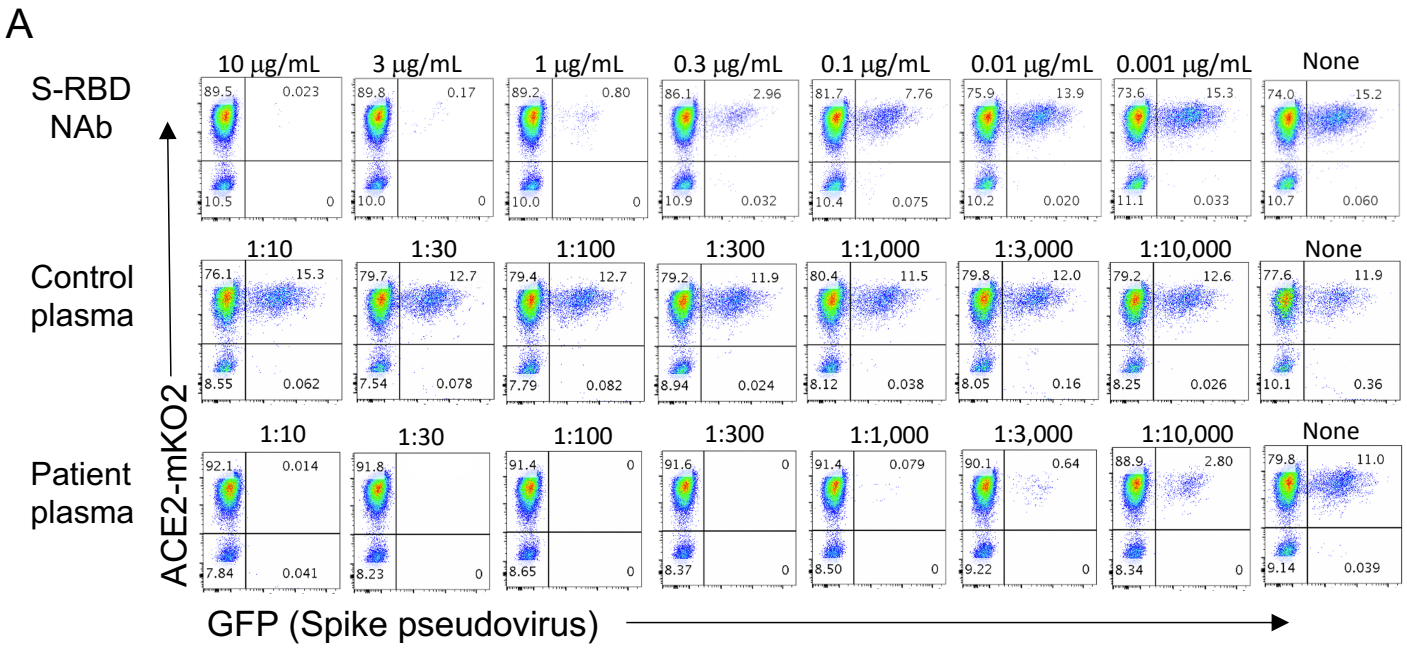

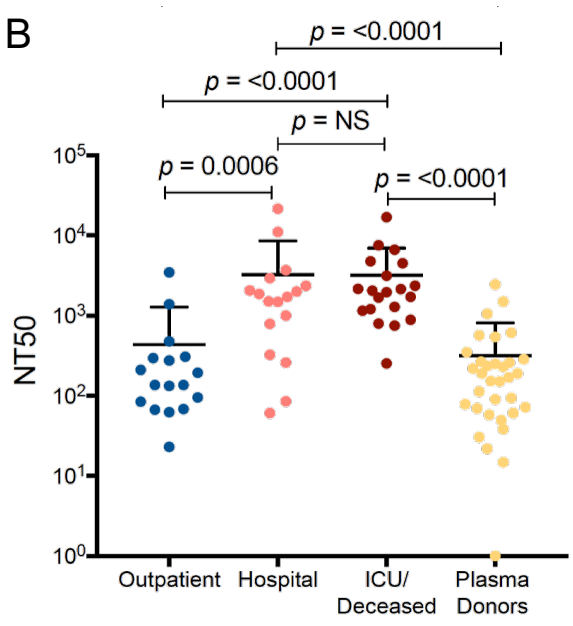

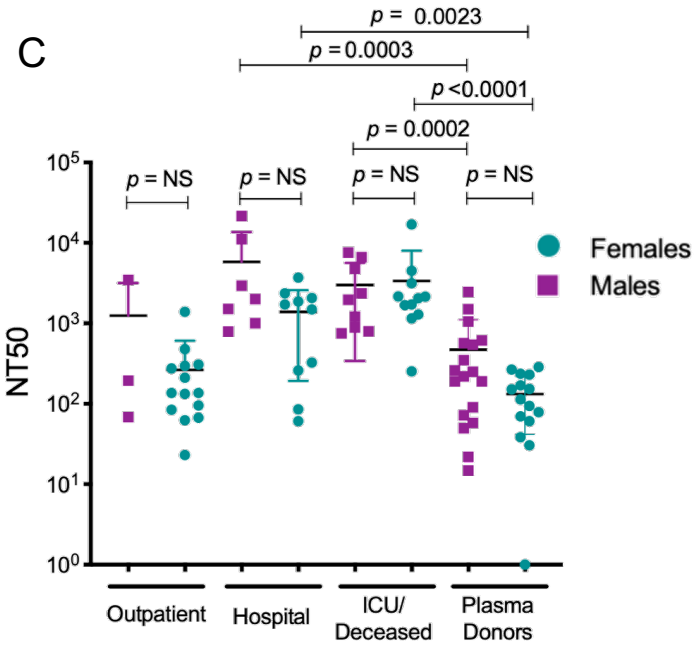

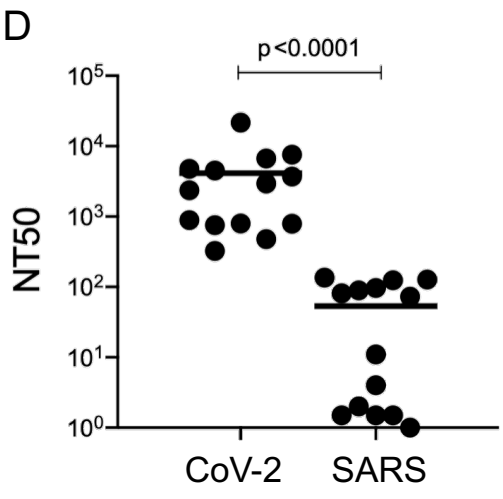

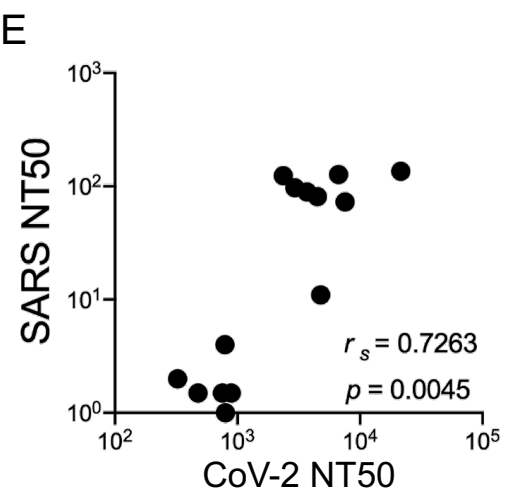

Fig. 5: Neutralizing titers for CoV-2 and SARS in COVID-19 subject plasma

a. Neutralization assay with S-RBD specific NAb, healthy control plasma, and a COVID-19 patient plasma. 3-fold serial dilutions of NAb from 10 μg/ml to 1 ng/ml or the plasma from 1:10 to 1:10,000 were pre-incubated with Spike protein pseudovirus and added to 293-ACE2 cells. GFP expression was analyzed by flow cytometry 3 days post infection. **b.** Neutralization titers (NT50) of COVID-19 plasma grouped as outpatient, hospitalized, ICU or deceased and convalescent plasma donor groups. **c.** NT50 of COVID-19 patient and plasma donor groups subdivided into males and females. **d.** Comparison of NT50 of COVID-19 plasma for CoV-2 and SARS neutralization. CoV-2 or SARS pseudoviruses were pre-incubated with COVID-19 plasma from hospitalized patients (n=14), 293-ACE2 cells were infected and RFP expression was determined at day 3 using flow cytometry. **e.** Correlation between the CoV-2 and SARS neutralization levels from same COVID-19 plasma. Two-tailed Mann-Whitney U test was used to determine the statistical significances in figures **b**, **c** and **d** and two-tailed Spearman's was used for figure **e**.

Figure 6

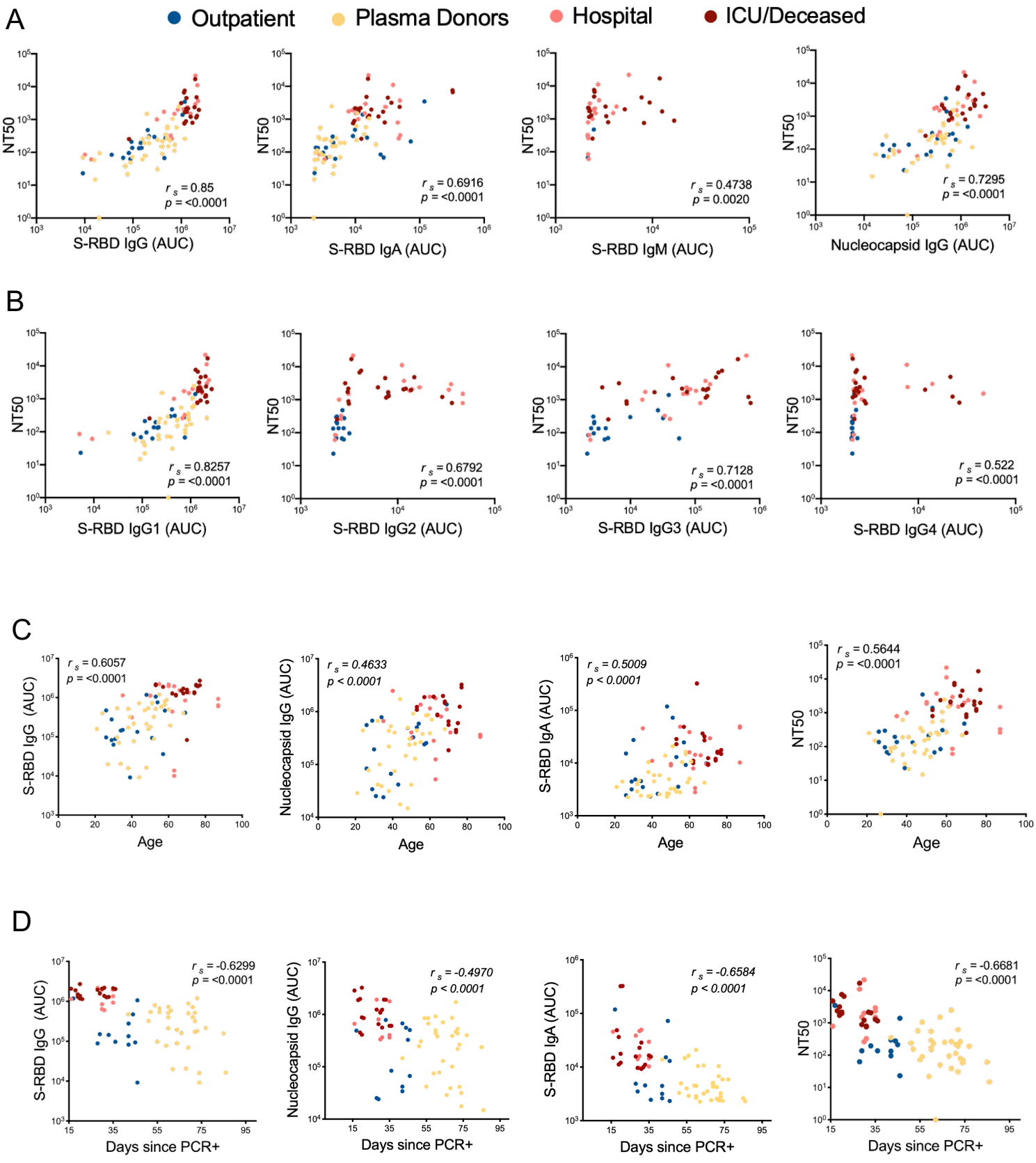

Fig. 6: Correlations of antibody, neutralization levels and COVID-19 subject characteristics

a. Neutralization (NT50) of COVID-19 plasma correlated with S-RBD IgG, S-RBD IgA, S-RBD IgM and Nucleocapsid IgG. **b.** Correlation of NT50 with S-RBD specific IgG subclasses; IgG1, IgG2, IgG3 and IgG4. **c.** Correlation of S-RBD IgG, Nucleocapsid IgG, S-RBD IgA and NT50 with Age. **d.** Correlation of S-RBD IgG, Nucleocapsid IgG, S-RBD IgA and NT50 with the number of days between PCR confirmation and the blood draw. Two-tailed Spearman's was used to determine statistical significances.

Supplementary Figure 1

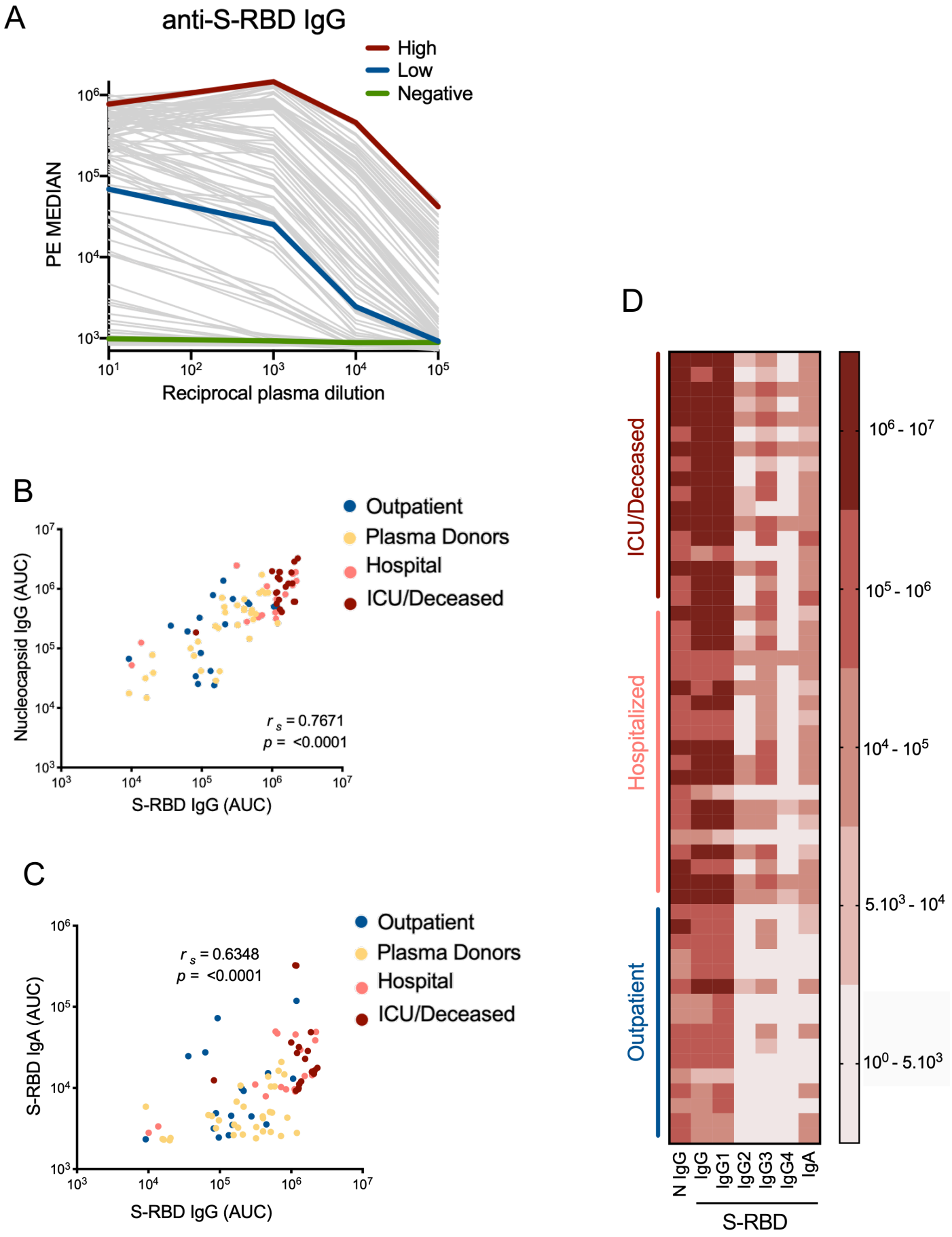

Supplementary Figure 1. SARS-CoV-2 S-RBD antibody detection

a. Antibody assay measuring the plasma reactivity to S-RBD. Flow cytometry analysis of the PE fluorescence conjugated to anti-human Ig antibody recognizing antibodies, present in the patient plasma and bound to S-RBD protein on the beads. Means of PE values in reciprocal dilutions were used to generate a curve for each positive plasma. Subject plasma with high and low antibody levels and a healthy control plasma were color-coded. **b.** Correlation of Nucleocapsid IgG with S-RBD IgG. **c**. Correlation of S-RBD IgA with S-RBD IgG. Two-tailed Spearman's was used to determine statistical significance. **d**. Heat map represents AUC values of Nucleocapsid (N) protein IgG, S-RBD IgG, S-RBD IgG subclasses and S-RBD IgA antibodies from individual subjects clustered as outpatients, hospitalized and ICU or deceased.

Supplementary Figure 2

A

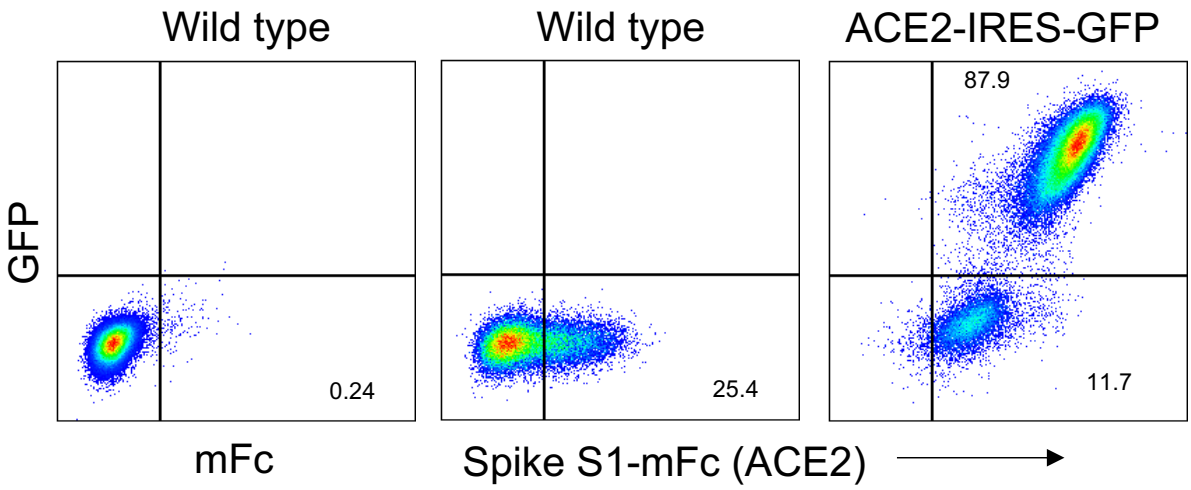

B

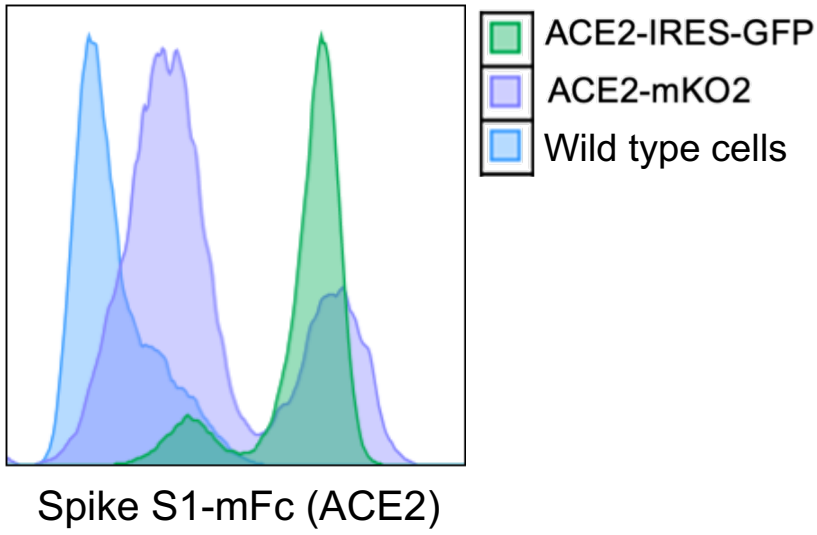

Supplementary Figure 2. ACE2 detection on cell surface membrane

a. Wild type or ACE2-IRES-GFP over-expressing 293 cells were stained with CoV-2 S1 protein, fused to mouse Fc, and anti-mouse Fc secondary antibody. **B**. ACE2 expression, detected as in **a**, in wild type and ACE2 overexpressing 293 cells compared in an overlay of flow data.

Supplementary Figure 3

A

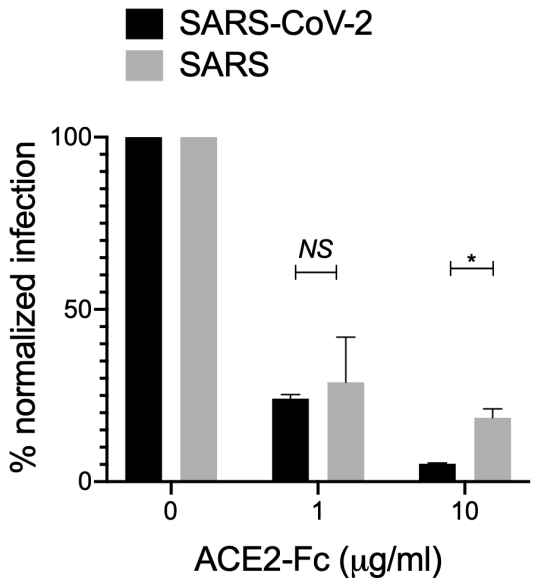

B

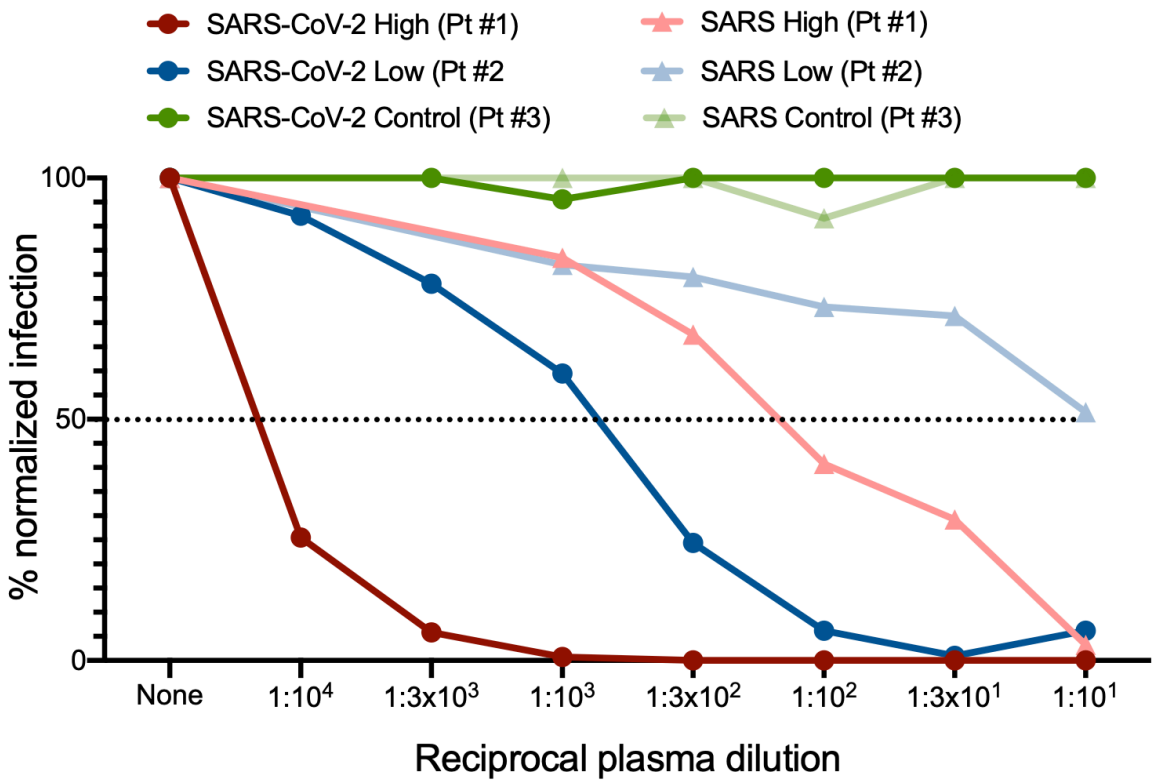

Supplementary Figure 3. Neutralization of CoV-2 and SARS pseudoviruses

A. Normalized percent infection levels of CoV-2 and SARS pseudoviruses in neutralization assay using soluble ACE2 at 1 μg/mL and 10 μg/ml concentrations. Significance was determined using two-tailed Mann-Whitney U test. **b.** Neutralization of CoV-2 and SARS pseudoviruses using subject plasma with high, low or no antibodies. Plasma were 3-fold serially diluted from 1:10 to 1:10.000. 3 different subject plasma were color-coded as examples. Infection percentages were normalized based on the infection levels of conditions in which no plasma was added.

Supplementary Figure 4

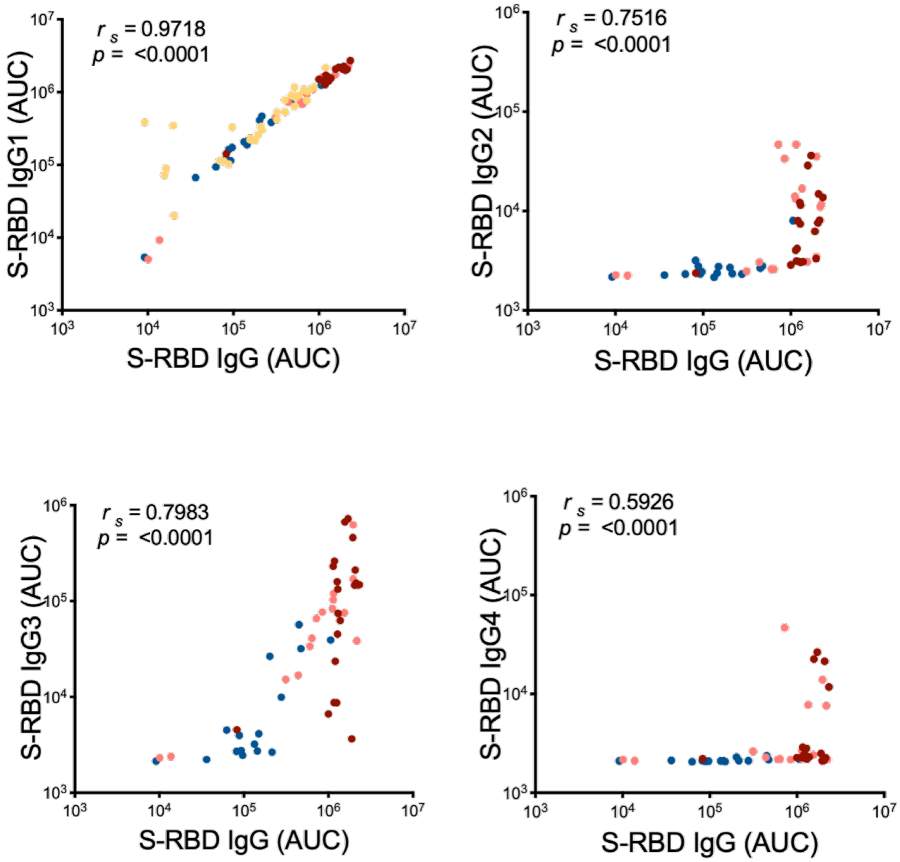

Supplementary Figure 4. S-RBD IgG subclasses correlation with total S-RBD IgG

A. Correlation of AUC levels of S-RBD specific IgG subclasses (IgG 1-4) with S-RBD specific total IgG. Two-tailed Spearman's was used to determine the statistical significance.